JAAS

Accepted Manuscript

This is an *Accepted Manuscript*, which has been through the Royal Society of Chemistry peer review process and has been accepted for publication.

Accepted Manuscripts are published online shortly after acceptance, before technical editing, formatting and proof reading. Using this free service, authors can make their results available to the community, in citable form, before we publish the edited article. We will replace this *Accepted Manuscript* with the edited and formatted *Advance Article* as soon as it is available.

You can find more information about *Accepted Manuscripts* in the Information for Authors.

Please note that technical editing may introduce minor changes to the text and/or graphics, which may alter content. The journal's standard Terms & Conditions and the Ethical guidelines still apply. In no event shall the Royal Society of Chemistry be held responsible for any errors or omissions in this *Accepted Manuscript* or any consequences arising from the use of any information it contains.

ROYAL SOCIETY OF CHEMISTRY

www.rsc.org/jaas

Iron speciation in soda lime silica glass: a comparison of XANES and UV-vis-NIR spectroscopy

Andrea Ceglia[a,b,c,*], Gert Nuyts[d], Wendy Meulebroeck[b], Simone Cagno[e,f], Alberta Silvestri[g], Alfonso Zoleo[h], Karin Nys[c], Koen Janssens[d], Hugo Thienpont[b], Herman Terryn[a]

[a]*Department of Electrochemical and Surface Engineering, SURF research group, Vrije Universiteit Brussel, Pleinlaan 2, B-1050 Brussels, Belgium*
[b]*Department of Applied Physics and Photonics, Brussels Photonics Team B-PHOT, Vrije Universiteit Brussel, Pleinlaan 2, B-1050 Brussels, Belgium*
[c]*Department of Art Sciences and Archaeology, MARI research group, Vrije Universiteit Brussel, Pleinlaan 2, B-1050 Brussels, Belgium*
[d]*Department of Chemistry, AXIL research group, Universiteit Antwerpen, Groenenborgerlaan 171, 2020 Antwerp, Belgium*
[e]*SCK-CEN, Belgian Nuclear Research Centre, Boeretang 200, 2400 Mol, Belgium*
[f]*CERAD, Norwegian University of Life Sciences, PO Box 5003, 1432 Ås, Norway*
[g]*Dipartimento di Geoscienze, Università di Padova, via G. Gradenigo 6, 35131, Padova, Italy*
[h]*Dipartimento di Scienze Chimiche, Università di Padova, via Marzolo 1, 35131, Padova, Italy*

Abstract

Scientific analyses of ancient glasses have been carried out for many years using elemental chemical analysis. However, it is known that the control of the redox conditions in the glass melt have a strong implication on the final hue of glass because it affects the $Fe^{2+}/\Sigma Fe$. Therefore an increasing number of studies of the redox conditions have been published in the recent years by means of synchrotron based X-ray absorption spectroscopy. This is a technique which is not easily accessible and requires dedicated facilities. In this paper we describe an alternative approach by means of optical absorption spectroscopy. We synthesised 10 soda-lime-silica glasses with known redox conditions and iron concentration to calibrate the absorption at 1100 nm in function of Fe^{2+} concentration. The linear extinction coefficient is also determined. These glasses were also studied by means of X-ray Absorption Near Edge Structure (XANES) spectroscopy. Electron Paramagnetic Resonance spectroscopy is additionally used as ancillary method to verify the quality of our data. Furthermore 28 samples from real archaeological samples were analysed with XANES and optical spectroscopy as a case study. The $Fe^{2+}/\Sigma Fe$ values obtained are compared and demonstrate that the two techniques are in good agreement. Optical spectroscopy can be applied in situ with moderate sample preparation to determine the concentration of Fe^{2+}. To investigate the redox conditions, especially as a first screening approach, this methodology is an important tool to take in consideration before applying more sophisticated techniques such as XANES, which is more elaborate and requires high-tech resources.

Keywords: Glass, UV-vis-NIR spectroscopy, XANES, EPR, archaeometry

1. Introduction

The recent years have seen a considerable increase of the applications of synchrotron based techniques to artistic and archaeological materials [1]. In particular, synchrotron X-rays Near Edge Absorption Structure (XANES) spectroscopy has become very popular in glass archaeometry [2–13]. This technique is useful because it allows to study the oxidation state and coordination geometry of metal ions in glass which determine its final hue. The control of furnace conditions and the choice of raw materials are known ways to tune the final hue of the glass [7]. XANES has been successfully applied to study the ratio between Fe^{2+} and Fe^{3+}, which is considered a marker for the redox state of natural and man-made silicate melts [5, 7, 14, 15]. Ancient glass typically contains between 0.3 wt% and 3 wt% of Fe_2O_3 introduced into the batch as a sand impurity [16]. Depending on its oxidation state, iron imparts different colours from yellow to green to blue. Fe^{3+} absorbs strongly in the UV and weakly at 380 nm, 420 nm and 440 nm, giving glass a yellow colour, Fe^{2+} absorbs in the near infrared at 1100 nm and its band tails in the visible generating the blue colour [17]. Different shades of colour can be obtained by mixing the two absorbing species. Early glassmakers made various attempts to control the hue by adding oxides of polyvalent metals, including manganese, antimony and, in the early modern period, arsenic [18]. Almost all the glasses produced in Roman and Late-Roman times are soda-lime silicate glasses. The variation of the ratio between major and minor oxides allowed scholars to identify few major compositional

*Corresponding author
Email address: aceglia@vub.ac.be, and.ceglia@gmail.com (Andrea Ceglia)

groups circulating in the first millennium AD (see [16] for more information).

This work was performed within the framework of a feasibility study of the application of UV-vis-NIR transmission spectroscopy to the archaeometric research on ancient glass. The aim of this paper is to compare the estimation of Fe^{2+} by means of XANES and UV-vis-NIR transmission spectroscopy for their application in archaeometry. The Fe K-edge and optical absorption spectroscopic signatures of iron in glass depend on the glass composition [19–21]. The application of XANES and UV-vis-NIR spectroscopy to samples of variable composition requires some assumptions. The first one is that the ratio of tetrahedrally and octahedrally coordinated Fe^{2+} and Fe^{3+} cations remains constant for all samples and calibration glasses; the second one is that the Fe^{2+} extinction coefficient at 1100 nm remains unchanged and depends only on the concentration of Fe^{2+} with no significant contributions from other species. Since it is impossible to cover all the ancient glass compositions, we prepared iron doped soda lime silica glasses to model an average "ancient-like" composition using the facilities of the glass company AGC Glass Europe. We aimed at a base composition similar to the Roman and Late Antique glass circulating in the Mediterranean area between the 1st and the 8th century AD. Specifically, this work targets glasses which are not intentionally coloured and iron was added as impurity of the sand [16].

To quantify the amount of $Fe^{2+}$and Fe^{3+}on the model glasses, wet chemistry and Electron Paramagnetic Resonance (EPR) were performed at the University of Padova, while XANES spectroscopy is applied as an independent method to quantify $Fe^{2+}/\Sigma Fe$. The values obtained by wet chemistry were used to calibrate the intensity of UV-vis-NIR absorption spectra to variable concentrations of Fe^{2+} in glass. Once the calibration of optical spectroscopy was accomplished, this was applied along with XANES to determine the redox state of iron in 28 glasses excavated from the Roman villa of Treignes, Belgium, and from the Late-Roman basilica of Ayoi Pente in Yeroskipou, Cyprus. This set of glasses is representative of the major compositional groups circulating in ancient Europe and of the variability within $Fe^{2+}/\Sigma Fe$ and total amount of iron found in Roman glass. In the context of this paper, the analysis of archaeological glasses has the purpose of evaluating the agreement between UV-vis-NIR and XANES spectroscopy.

2. Material

2.1. Model glass

In collaboration with the R&D department of AGC Glass Europe we prepared two series of five iron doped soda-lime-silicate glasses. The first set, hereafter referred to as Fe-series, has a base composition of 3 wt% Al_2O_3, 8 wt% CaO and 15 wt% Na_2O and Fe_2O_3 varying from 0 to 0.8 wt%. The second series, named R-series, has the same base composition but Fe_2O_3 was kept stable at about 0.55 wt% and, by adding $NaNO_3$ or carbon, respectively oxidising and reducing conditions were applied.

Both series were manufactured following the same procedure: raw materials were melted in a Pt crucible in an inert N_2 atmosphere for 6 hours at 1550 °C. After two and four hours the glass was poured, broken and remelted for homogenisation and after six hours it was poured in a 4x4 cm^2 frame and polished to 4 mm thickness.

For all glasses, AGC glass Europe provided the chemical composition by means of a WDS-XRF S4 Pioneer X-Rays Fluorescence (XRF). The data are reported in Table 1. Nevertheless, for the R-series only iron and sulphur were measured since the base glass composition is the same of sample R3.

2.2. Archaeological glass

In addition to the lab-made model glasses we analysed 28 fragments from two real ancient contexts. The first is the archaeological site of Treignes, Belgium, where the Roman villa "les Bruyres" was excavated and several glass fragments were found. The villa dates from the late 3rd to the beginning of the 5th century AD. The chemical composition of the glasses is reported in another paper [22].

The second site is the Early Christian Basilica of Ayoi Pente in Yeroskipou, Cyprus [23]. The site came to light during road works and got heavily damaged by bulldozing, tomb robbing and ploughing. The basilica is dated between the 5th and the 7th century and much of the excavated glass can be attributed to lamp and window fragments. The archaeometric study of the glass excavated in this basilica is presented elsewhere [24]. For the full chemical composition and the quantification methodology the reader is directed to the cited literature [22, 24]. In this paper we report only the values of total iron obtained by Electron Probe Micro Analyser (EPMA).

These glass fragments presented variable degree of corrosion, typically iridescence layers or salt crusts. To carry out optical measurements, we have polished an area of a few millimetres diameter with a hand-held rotary tool to eliminate the corrosion layers that would strongly affect the transmission of light [25]. In addition, all fragments studied here were sampled, embedded in resins and polished for chemical analysis. The same resins were used for XANES measurements.

3. Experimental

3.1. Total amount of iron

The techniques employed give complementary information. Whilst optical absorption spectroscopy quantifies the weight percentage of Fe^{2+} ions, EPR is correlated to the absolute amount of Fe^{3+} ions and XANES provides the ratio $Fe^{2+}/\Sigma Fe$ in percentage without absolute quantification. Hence, the total amount of iron is an important parameter to determine quantitatively both Fe^{2+} and Fe^{3+}

with these methods. For the Fe- and R- series total iron was measured by XRF at AGC Glass Europe. Archaeological glasses were chemically analysed using a CAMECA SX-FIVE EPMA equipped with a LaB_6 gun, 5 WDS spectrometer and an EDS Bruker. Quantitative measurements were acquired employing a two-run procedure where we changed current and counting times, while acceleration voltage and beam diameter were kept at 15 kV and 40 μm respectively. For Si, Na, K, Al, Mn, Cl, Mg, Cu, Fe and S, beam current was set at 20 nA and counting times were 10 seconds both on the sample and the background (except for Na, Si and K for which we measured for 3 seconds on the peak to avoid alkalis displacement) [24]. For minor elements (Cu, Sb, Co, Pb, Zn, P, Ti and Ba) the beam current was set at 300 nA and counting time was 30 seconds on the peak (60 seconds for Zn and Cu) and 10 seconds on the background. We used several mineral and metallic standards: albite (Na, Al, Si), pyroxene (Mg, Ca), pyrite (S), scapolite (Cl), orthoclase (K), haematite (Fe), pyrophanite (Mn,Ti), apatite (P), cobalt (Co), copper (Cu), zinc sulphide (Zn), stibnite (Sb), barium sulphate (Ba) and galena (Pb).

3.2. Wet chemistry

The amount of Fe^{2+} in the model glasses provided by AGC Glass Europe was determined by titration with potassium permanganate using the Pratt and Washington method [26]. The analytical procedure is reported in detail in [27]. The results were checked against international standards (AL-I Albite; FK-N K-feldspar; NIM-S Syenite; JR-2- Rhyolite). Their certified values are reported in [28] and Fe^{2+} contents are comparable to those of our model glass samples (ranging from 0.03 to 0.30 Fe^{2+} wt%). Precision of the measures is about 10% for Fe^{2+} contents < 0.10 wt% and about 5% for contents > 0.10 wt%. Accuracy is within 10%, independently of Fe^{2+} content. Results of titration with potassium permanganate for the model glasses are reported in Table 2.

3.3. Electron Paramagnetic Resonance

Continuous wave EPR (CW-EPR) spectra were acquired on powdered samples with a Bruker ECS instrument equipped with a TE102 cavity. All the CW-EPR spectra were acquired under the same instrumental conditions (microwave power 2.0 mW, modulation amplitude 0.5 mT, microwave frequency 9.55 GHZ, T=300 K). Before every acquisition, each sample was weighed, placed in the same EPR quartz tube and located in the same position inside the resonator. The EPR signal is due to paramagnetic species, therefore only the absolute amount of Fe^{3+} iron can be detected with this technique. Fe^{2+} is determined subtracting the ferric fraction from the total amount of iron. The fitting method and the calibration line for Fe^{3+} was shown previously [29]. Shortly, the method is based on a fitting function $w \cdot f(C_{Fe^{3+}})$ where w is a weight factor and $f(C_{Fe^{3+}})$ is the EPR spectrum of 1 mg glass sample of known concentration $C_{Fe^{3+}}$. A Least Squares algorithm finds the best w value and the amount of Fe^{3+} in the sample is then calculated as $w \cdot C_{Fe^{3+}}$ divided by the sample weight.

3.4. X-ray Absorption Near Edge Structure (XANES)

The Fe-K edge XANES measurements were performed at European Synchrotron Radiation Facility (ESRF), in the Belgian-Dutch beamline (DUBBLE) BM26A, Grenoble (France). A Si(111) double crystal monochromator was used, having an energy resolution $\Delta E/E$ of about 10^{-4}. A transmission XANES spectrum was recorded from a metallic Fe reference foil (7.5 μm) and used to provide an accurate energy calibration for all spectra; the first inflection point of the Fe-K edge was set to 7112 eV [30]. Higher harmonics are removed from the incident beam by two mirrors, one before and one after the monochromator, each with a Si and Pt strip. The former is used for energies lower then 12.5 keV and the latter for energies higher than 12.5 keV. The reference compounds $FeSO_4 \cdot 7\,H_2O$ ($^{[6]}Fe^{2+}$), hercynite ($^{[4]}Fe^{2+}$), chromite ($^{[4]}Fe^{2+}$), epidote ($^{[6]}Fe^{3+}$) and aegerine ($^{[6]}Fe^{3+}$) provided reference transmission spectra for ferrous and ferric iron. The powdered compounds were diluted with PolyVinyl Chloride (PVC) pressed into a pellet. In order to obtain an absorption jump of about 1, the amount of compound and PVC were calculated using Absorbix [31]. To avoid contributions of possible heterogeneities during mixing, the reference XANES spectra were recorded with an unfocused beam (1x5 mm^2).

The thickness of archaeological and model samples prevents transmission XANES measurements, thus the spectra were obtained by monitoring the fluorescence intensity as a function of the excitation energy. XANES signals were recorded with the sample oriented at 45° to the incident beam. The fluorescence yield was collected using a Vortex Silicon Drift Detector (SDD) at an angle of 45° with respect to the sample surface.

All the spectra were recorded on the bulk of the samples and they were collected from 6845 eV to 7570 eV using different energy intervals and measuring times (6845 eV - 7090 eV: 10 eV, 1 s; 7090 eV - 7145 eV: 0.2 eV, 3 s; 7145 eV - 7570 eV: linearly decreasing data point density up to a maximum interval of 4.5 eV at 7570 eV, while the measuring time increases from 5000 ms to 30 s.), resulting in $\sim$ 1 hour measuring time per XANES spectrum. During a previous beam time in HASYLAB beamline L, we measured for 20 minutes using a 780x520 μm^2 beam and no photo-reduction occurred [7]. At DUBBLE we measured the pre-edge region for $\pm$8 minutes with a 1x5 mm^2 beam and a comparable flux (10^{11}) that assures us to avoid any beam damage.

For all XANES spectra,the normalisation was performed by using in-house written Matlab software. An edge-step normalisation was performed by a first-order pre-edge subtraction and by regression of a second-order polynomial beyond the edge. [32]

The analysis of the pre-edge allows to draw conclusions on the redox state of iron and its coordination chemistry. The pre-edge peak is extracted using an arctangent function, describing the background, then it has been fitted using two Voigt peaks, constrained to have a 50% Lorentzian 50% Gaussian shape, with a resulting average width of 2 eV [7]. Fitting was carried out using Igor Pro software.

It is well described in literature that the centroid energy of the pre-edge correlates linearly with the $Fe^{2+}/\Sigma Fe$ ratio of iron in glass [14]. The centroid is calculated by the following formula:

$$\text{centroid (eV)} = \frac{P_1 \cdot A_1 + P_2 \cdot A_2}{A_1 + A_2}$$

where P_1 and P_2 are the peak positions (eV) and A_1 and A_2 the normalised peak areas of the respective Voigt functions. Since the centroid is linked to the $Fe^{2+}/\Sigma Fe$ ratio, we can calculate the ferric and ferrous component knowing the total concentration of iron. To evaluate the error on the centroid we carried three independent measurements on each model glass and the centroid values were found to be always within 0.01 eV. However, taking into account the error on all fitted parameters and applying the error propagation, we calculated a final error of ±0.07 eV on the centroid and we estimated an error smaller than ±0.01 arbitrary unites on the integrated area.

3.5. UV-vis-NIR spectroscopy

The set-up for optical spectroscopy consists of two light sources, a 30-W deuterium lamp emitting in the UV spectral region and a 20-W halogen lamp emitting visible and infrared light. The sources are connected to an optical fibre which brings the light on a plano-convex focusing lens. The light is focussed at the entrance of an integrating sphere which collects the transmitted light and through an optical fibre transfers it to the spectrometer, a SA320 Instrument Systems optical spectrum analyser. Although the SA320 is a not a portable spectrometer, it was previously demonstrated that the same results could be obtained with a compact mobile module of two spectrometers, the AvaSpec-3648 and the AvaSpec-256-NIR1.7 from Avantes [33]. All model glasses were measured with both SA320 and the Avantes spectrometers. In addition, some spectra of the samples of Yeroskipou were recorded *in situ* at the Paphos District Museum in Cyprus and, when sampled for chemical analysis, remeasured with the laboratory SA320 spectrometer.

Transmission spectra were recorded between 300 and 1650 nm with a spectral resolution of 1.5 nm. The spot diameter on the sample is between 3-4 mm. The integrating sphere has an aperture of 6 mm and allows the collection of all transmitted light, reducing the effects of the curvature of the glass fragments and eventual polishing defects. In order to quantitatively interpret optical spectra, they have to be normalised (to 1 mm of thickness) and losses due to Fresnel reflections at the surfaces must be subtracted. The removal of reflection losses was approximated using an average refractive index of 1.5 and considering that the maximum incident angle is 20°, the average reflectance is R=0.04 at each surface (for more details see [17]). For the normalisation, we measured the thickness using a digital micrometer with 0.001 mm resolution. Ancient glasses have a variety of forms and they might not always offer parallel surfaces for the analysis. However, in archaeological context, findings are often fragments and it is easy to pinpoint a relatively flat area. From our experience, the variation in thickness is limited within the spot size of less than 4 mm and we estimated (actually overestimated) its variability to be ±0.1 mm. These values will be used to calculate the error on the determination of Fe^{2+}.

In soda-lime-silica glasses Fe^{2+} has a broad absorbtion band at around 1100 nm [17, 34, 35]. Therefore the calibration curve for Fe^{2+} in glass is built using the absorption at this wavelength for the glass of the AGC Fe- and R-series through the Lambert-Beer law:

$$\mathrm{A}_{1100nm} = \epsilon \cdot d \cdot C_{Fe^{2+}}$$

where ϵ is the linear absorption coefficient of Fe^{2+}, d is the thickness of the glass fragment and $C_{Fe^{2+}}$ is the concentration of Fe^{2+} in elemental wt%. For the archaeological glasses, the $Fe^{2+}/\Sigma Fe$ was calculated using the EPMA quantification for total iron and the Fe^{2+} value obtained by means of optical spectroscopy.

4. Results

In order to keep the structure easy to follow for the reader, we have split this section in two. The first part will concern the model glass. We will show the results obtained by each technique and will compare them to the values determined by wet chemistry. In the second part we will report the data obtained by XANES and optical spectroscopy on archaeological samples excavated in a Roman villa from Treignes, Belgium, and the Late Antique basilica of Ayoi Pente in Cyprus.

4.1. Calibration procedure: the model glasses

In Table 2 we report the values in elemental wt% of Fe^{2+} concentration determined by wet chemistry and the quantification with XANES and EPR. Additionally, we provide the absorbance values at 1100 nm ($\mathrm{A}_{1100\mathrm{nm}}$) used for the calibration of optical spectroscopy and the centroids calculated on the XANES spectra. The values of Fe^{2+} determined by UV-vis-NIR spectroscopy are recalculated using the calibration curve. The Fe-series was manufactured in order to have similar $Fe^{2+}/\Sigma Fe$ and increasing total amount of iron. On the contrary, the R-series was made with different redox conditions applied in order to vary the $Fe^{2+}/\Sigma Fe$ ratio. In the following paragraph we report the quantification of the redox state of iron by EPR and XANES, and details about the application of optical spectroscopy to the model glasses.

4.1.1. Electron Paramagnetic Resonance

EPR is a reference technique for the determination of the absolute amount Fe^{3+} iron. Figure 1 shows the spectra obtained on the Fe-series. The spectra are characterised by an intense feature at g = 4.23 (160 mT) and a smaller one at g = 2 (300 mT). The former is due to Fe^{3+} in sites with low symmetry, while the latter is related to sites at higher symmetry. In general, there is consensus that in alkali lime silica glasses almost all the Fe^{3+} is in tetrahedral site, replacing the Si^{4+} in the network. Due to the different valence of Si^{4+} and Fe^{3+}, a monovalent cation is required in proximity to iron to guarantee electroneutrality. The types of cations (H^+, Li^+, Na^+) and the specific position with respect to Fe^{3+}, affect the electronic symmetry around Fe^{3+}. The lower the symmetry the stronger the line at g = 4.23 [36]. In the inset, we show a zoom of the spectra of samples R3 and R4. The spectra of these glasses show a feature at g = 2.175 (312 mT) that does not occur in other samples. At present, this remains unexplained.

The data are fitted as explained in [29] to calculate the concentration of Fe^{3+} and since we know the total amount of Fe (Table 1), we can calculate the amount of Fe^{2+} iron as well. The values obtained are reported in Table 2.

4.1.2. XANES

It is well known that the energy of the absorption edge of transition elements shifts to higher energies, increasing the oxidation state [37]. The position of the K-absorption edge of iron behaves accordingly. Figure 2 shows the evolution of the XANES profiles of samples R1, R3 and R5, which are changing from oxidised to reduced. The graph exhibits very well the progressive shift of the edge towards higher energy. The inset offers a detailed view on the pre-edge peak, which allows a better quantitative analysis. After background subtraction and fitting, we have calculated the centroid which is a good indicator of the $Fe^{2+}/\Sigma Fe$. The centroid shifts from 7112.90 eV for the R5, the most reduced, to 7113.68 eV for R1, the most oxidised. We have analysed all samples of the R-series and two samples from the Fe-Series (Fe3 and Fe4).

The average centroid value for ferrous reference compounds ($FeSO_4 \cdot 7\,H_2O$, hercynite and chromite) is 7112.47 eV, while for ferric compounds (epidote and aegerine) it is 7114.05 eV. In Table 3 we report the centroid position and the area of the pre-edge for each reference analysed. Besides the mineral compounds we measured also two reference glasses with known $Fe^{2+}/\Sigma Fe$. ST1 is a soda-lime-silicate glass which was made by the Stazione Sperimentale del Vetro and contains about 33% of ferrous iron [8, 12, 38]. SRM1830 is a soda-lime-silica glass manufactured by the National Institute of Standards and Technology (NIST) containing 30% of Fe^{2+}. We have fitted a linear curve through the references in order to build a mathematical relationship between $Fe^{2+}/\Sigma Fe$ and the centroid. Figure 3 reports the linear fit of the relation between the centroid obtained for Fe^{2+} and Fe^{3+} reference compounds and the iron redox ratio. When we plot also the glasses of the Fe- and R-series using the $Fe^{2+}/\Sigma Fe$ values obtained by wet chemistry, we see that samples lie along the correlation line, with the exception of sample R4. This means that a linear correlation between the centroid and the $Fe^{2+}/\Sigma Fe$ can be assumed to be correct. In Table 2 for the XANES measures we report the values of Fe^{2+} calculated using the following correlation:

$$Fe^{2+}/\Sigma Fe_{tot} = \frac{\text{Centroid (eV)} - 7114}{-1.529}$$

4.1.3. UV-vis-NIR spectroscopy

In order to obtain the linear extinction coefficient, the UV-vis-NIR response at 1100 nm needs to be calibrated, using the reference glasses of the Fe- and R-series with known Fe^{2+} wt%. In Figure 4 we report the correlation line between optical absorption at 1100 nm per mm of glass thickness and Fe^{2+} (in elemental wt%). The regression between the values obtain by wet chemistry and optical spectroscopy is good (r^2=0.979). The slope of the correlation line in Figure 4 is the linear extinction coefficient ϵ = 1.23±0.06 $wt\%^{-1}mm^{-1}$ (27.5±1.5 L $mol^{-1}cm^{-1}$, assuming a density of 2.5 g/cm^3) which is similar to published data for silica glasses [17, 34, 39]. Such correlation will be used to analyse ancient glass and determine their redox state.

4.2. Case study: the archaeological glasses

The archaeological glass available for this study was analysed by XANES and UV-vis-NIR in order to quantify $Fe^{2+}/\Sigma Fe$. In Supplementary Table we report the $Fe^{2+}/\Sigma Fe$ ratio and the Fe^{2+}‘ concentration calculated by XANES and optical spectroscopy. Additionally we provide the centroid energies of the pre-edge, the absorbance at 1100 nm (A_{1100}) and the total amount of iron measured by EPMA. Figure 5 shows the quantification of Fe^{2+} obtained by XANES and UV-vis-NIR spectroscopy on the material from Treignes and Yeroskipou. A line with slope 1 is also shown and, if we remove two outliers (YER1_10 and YER8_1), the relation is quite good (r^2=0.961) with respect to the bisector. The horizontal error bars are calculated applying a ±0.07 eV uncertainty on the centroid position. Vertical bars are determined by considering a ±0.1 mm variability on the thickness used to normalise the optical spectra (on samples YER1_10 and YER8_1 the error estimated is incorrect as there was no transmission at 1100 nm.).

5. Discussion

The study of redox ratio of iron in glass is very useful to investigate the melting conditions. It can be related to the chemistry of the starting materials or the furnace properties [7]. The results on model glasses and archaeological fragments showed clearly that both techniques, XANES and optical spectroscopy, offer a good quantification for Fe^{2+} and Fe^{3+} when the total amount of iron is

known. Using the Fe-series and R-series made by AGC Glass Europe we compared EPR and XANES, two independent methods for the determination of the $Fe^{2+}/\Sigma Fe$ ratio. The value obtained by these techniques are in good agreement with wet chemistry. Optical spectroscopy is particularly useful to study ancient glass since it can be applied *in situ* without a significant degradation of the signal [33]. Compared to EPR, UV-vis-NIR spectroscopy does not require large equipment, it is relatively simpler and it can be applied *in-situ*. XANES spectroscopy is non destructive too, without particular need of sample preparation (excluding the necessary steps required to avoid measuring a contaminated weathered surface), nevertheless it requires synchrotron facilities which are not easily accessible. Having a method that can be applied *in situ* with little sample preparation is an important advantage in the field of archaeological sciences. Furthermore, optical spectrometers are widely available in universities and research institutes.

EPR is a standard method for the quantification of Fe^{3+} in glass. The method was calibrated with other glass standards as reported in [29]. As shown in Table 2 the indirect determination of Fe^{2+} confirms the values obtained by wet chemistry. The amount of Fe^{2+} is determined subtracting the Fe^{3+} estimated by EPR from the total amount of iron measured by XRF.

The analysis of the pre-edge feature of iron by means of XANES spectroscopy allows the determination of the $Fe^{2+}/\Sigma Fe$ ratio independently from the total amount of iron. The relation between the centroid energy and the $Fe^{2+}/\Sigma Fe$ ratio was assumed linear as reported in previous literature [7, 14]. In order to obtain the calibration curve, we have analysed the pre-edge features of Fe^{2+} and Fe^{3+} reference compounds. Figure 3 shows that the AGC glasses analysed follow the calibration curve as expected. The only exception is sample R4, possibly due to inhomogeneity of this sample. This is also suggested by EPR spectroscopy. Samples R3 and R4 have a feature which does not occur in the other glasses (Figure 1).

5.1. Determination of Fe^{2+} by XANES and UV-vis-NIR

In this work XANES and UV-vis-NIR spectroscopy are compared to see whether the latter technique can be considered a source of reliable quantitative data for the study of transparent archaeological glass. First of all, we should assume that the peak at 1100 nm arises only from Fe^{2+} in order to apply the Lambert-Beer law to archaeological glasses. Although copper could have a minor contribution to the absorbance, this assumption is quite safe for this work. Copper in the oxidised state, Cu^{2+}, absorbs at about 790 nm in soda-lime-silica glass with an absorption coefficient of $\epsilon_{Cu^{2+}} = 15.7$ wt%$^{-1}$cm^{-1} (40 L mol^{-1}cm^{-1}) [40]. At 1100 nm Cu^{2+} absorption is lower, about 7.8 wt%$^{-1}$cm^{-1} (20 L mol^{-1}cm^{-1}). The aim of this paper is to model unintentionally coloured glasses, which contains only 10-50 ppm of copper. With 50 ppm of Cu^{2+} the absorbance is overestimated of 0.004, that is about 0.003 wt% of Fe^{2+}. The amount of copper might increase with recycling up to few thousands of ppm [41], still having only a very minor effect on the absorption at 1100 nm. Furthermore, only a minor part of the copper is in the oxidised state as ancient furnace conditions were generally reducing [5, 7]. For intentionally coloured glass, appropriate correction should be undertaken by fitting the respective contribution of Fe^{2+} and Cu^{2+}.

A second assumption that we have to make is that the ratio between tetrahedral and octahedral coordinated iron is the same for all samples and calibration glasses. Whether or not this can be taken for granted was checked by studying the pre-edge of XANES spectra. The pre-edge is due to the $1s \rightarrow 3d$ transition and is influenced by the oxidation state. This determines the centroid position, and the coordination geometry, which has an influence on the intensity of the transition. Normally the $1s \rightarrow 3d$ transition is forbidden by the selection rules ($\Delta l = \pm 1$), but in distorted geometries, such as the tetrahedral coordination, a certain mixing between the 4p and 3d orbitals occurs and it increases the probability of this transition. The mixing of the orbitals does not happen in the octahedral coordination, hence the pre-edge has a much lower intensity. Therefore the integrated area of the pre-edge is higher for tetrahedral coordination compared to octahedral geometries. In order to study the change of tetrahedral ([4]) and octahedral ([6]) components in glass, we have plotted the area of the pre-edge against the centroid position in Figure 6. This type of graph was introduced by Wilke et al. [42] and it is generally used to determine the coordination and the redox state of iron. Besides our reference compounds, we show also the values obtained by Wilke et al. on similar reference minerals (see Table 3). The data from Wilke et al. are offset of 0.44 eV, which is the average energy difference between our centroids values and theirs. We actually would expect an energy shift of 0.92 since they calibrated the energy by setting the first inflection point of iron metal at 7111.08, while we used 7112 eV (as usually accepted). Both chromite and aegerine are tetrahedral ferrous minerals ($^{[4]}Fe^{2+}$), but their pre-edge peaks have different intensities. This probably occurs because of the presence of some octahedral sites in chromite [42]. All archaeological samples and the model glasses lie on a curve that connects the chromite to the tetrahedral Fe^{3+} coordination. Wilke et al. [42], and Jackson et al. [20] showed that this happens when all the samples have a constant $^{[4]}Fe^{2+}/^{[6]}Fe^{2+}$ and $^{[4]}Fe^{3+}/^{[6]}Fe^{3+}$ ratios. Therefore this can be assumed as valid for all archaeological glasses studied here.

5.2. Feasibility assessment of optical spectroscopy

Since the Fe and R series contained less than 0.3 wt% of Fe^{2+}, one may wonder whether the calibration of optical spectroscopy keeps valid also for higher Fe^{2+} concentrations. Fe^{2+} is underestimated by optical spectroscopy for samples YER1_10 and YER8_1. This occurs because these glasses are strongly coloured and relatively thick (about 2

mm). As a consequence the transmission of the light at 1100 nm is nearly null, affecting the accuracy of the data and the derived calculations. In Figure 7 we show the transmission spectra of the 4 samples with high Fe^{2+} content (>0.5 wt%). These spectra were neither corrected for reflection losses nor normalised for the thickness. Samples YER5_4 and YER5_1 are thin enough (about 1 mm) to transmit light at 1100 nm, while samples YER1_10 and YER8_1 are thicker (about 2 mm) and there is almost no light transmitted at 1100 nm. Consequently Fe^{2+} is underestimated in the latter samples, while it is correctly quantified in the other two samples. This observation lets us conclude that the calibration line for optical spectroscopy remains valid also outside the range of the Fe- and R- series provided that there is enough transmitted light.

The lower limit of detection (LOD) is determined by the calibration line we built. Values of Fe^{2+} lower the 0.01 wt% will produce no significant change in absorbance. The upper limit depends on the spectrometer, the measurements conditions and the sample itself. High end spectrometers have very limited stray light error and can measure the absorbance up to 3. However, to be sure that the linearity of the Bouguer Lambert Beer law is respected one should work in the range between 0.1-1.5 A. However, for *in situ* applications we used a less performing compact spectrometer. In addition, normally *in situ* the environmental conditions are not best and higher stray light reduces the maximum absorbance measurable. Therefore, we advice that the glass sample should transmit at least 5% of light (absorbance < 1.3) to carry out quantitative measurements. The maximum thickness of the sample that allows to collect reliable data depends on the Fe^{2+} concentration. For Fe^{2+} = 1 wt% the sample should not exceed 1 mm in thickness. Nevertheless, most of archaeological glasses have less than 0.3 wt% of Fe^{2+} (see Figure 5) which allows to measure confidently glass fragments with a thickness up to 3.5 mm.

There are specific applications in which XANES is preferred over UV-vis-NIR spectroscopy. When spatial resolution is required, certain synchrotron beamlines with micro optics allowed to study XANES spectra with micro or nano-resolution, which can be necessary for example to study degradation processes [6, 43]. When the glass is opaque or strongly coloured, as is the case of samples YER1_10 and YER8_1, XANES measurements are not hampered, while optical spectroscopy cannot be carried out on the samples without sample preparation. Indeed, it could be possible to make a very thin slide which would let pass enough light to collect reliable accurate spectra). Besides few cases in which optical spectroscopy might fail, our results show that this technique can certainly be used to quantify Fe^{2+} in archaeological glasses.

6. Conclusions

This paper demonstrates that optical spectroscopy is a valid technique to determine the concentration of Fe^{2+} in ancient soda lime silica glass. We have compared analytical results obtained by optical spectroscopy to XANES spectroscopy, which is often used to study the redox state of elements in glass and is considered a reference method. However, this technique is not easily accessible and requires dedicated facilities. Moreover, optical spectroscopy can be applied *in situ* allowing to determine the Fe^{2+} content of ancient glass with limited preparation of the surface and without the need of sampling the material. We applied these techniques on model glasses and archaeological samples from Roman and Late Roman contexts.

Optical spectroscopy gave nearly the same results than XANES spectroscopy as argued by the good correlation coefficient of determination (r^2=0.961). However, we do not want to state that optical spectroscopy can substitute XANES in all aspects of the archaeometric study of ancient glass. There are many differences between the two techniques that keep them as complementary tools. For several cases XANES is a preferential technique, *i.e.* deeply coloured or opaque glass, or when a higher spatial resolution should be required. On the other hand, we want to stress that to investigate the redox conditions, especially as a first screening approach, UV-vis-NIR spectroscopy is an important tool to take in consideration before applying more sophisticated techniques such as XANES, which requires longer time and high-tech resources.

7. Acknowledgements

The research leading to these results has received funding from the European Union Seventh Framework Programme FP7/2007-2013 under grant agreement n° 265010. For more information please visit the NARNIA website: `http://narnia-itn.eu/`. This work was partly supported by the Research Council of Norway through its Centres of Excellence funding scheme, project number 223268/F50. We are grateful to the ESRF for granting beamtime and Dipanjan Banerjee for his help at the beamline. We are thankful to the R&D department of AGC Glass Europe, in particular Dr Benoit Cherdon, Dr Dominique Michiels and Ms Dominique Delleuze, for preparing glass for us and providing us the chemical information. A special thanks to M. Fialin for the help with EPMA measurements in CAMPARIS. We want to express our gratitude to F. Farges and A. Berry for sharing their XANES spectra with us. Thanks to Anne Isabelle for reading this paper and giving these comments. Finally we are grateful to two anonymous reviewers who contributed to improve this paper.

References

[1] S. Quartieri, Synchrotron Radiation in Art, Archaeology and Cultural Heritage, in: S. Mobilio, F. Boscherini, C. Meneghini (Eds.), Synchrotron Radiation, Springer Berlin Heidelberg, 2015, pp. 677–695. `doi:10.1007/978-3-642-55315-8\_26`. URL `http://link.springer.com/chapter/10.1007/978-3-642-55315-8_26`

[2] M. Abuín, A. Serrano, J. Chaboy, M. A. García, N. Carmona, XAS study of Mn, Fe and Cu as indicators of historical glass decay, Journal of Analytical Atomic Spectrometry 28 (7) (2013) 1118. doi:10.1039/c3ja30374h.
URL http://pubs.rsc.org/en/content/articlehtml/2013/ja/c3ja30374hhttp://xlink.rsc.org/?DOI=c3ja30374h

[3] R. Arletti, G. Vezzalini, S. Quartieri, D. Ferrari, M. Merlini, M. Cotte, Polychrome glass from Etruscan sites: first non-destructive characterization with synchrotron μ-XRF, μ-XANES and XRPD, Applied Physics A 92 (1) (2008) 127–135. doi:10.1007/s00339-008-4462-x.
URL http://www.springerlink.com/index/10.1007/s00339-008-4462-x

[4] R. Arletti, C. Giacobbe, S. Quartieri, G. Sabatino, G. Tigano, M. Triscari, G. Vezzalini, Archaeometrical Investigation of Sicilian Early Byzantine Glass: Chemical and Spectroscopic Data*, Archaeometry 52 (1) (2010) 99–114. doi:10.1111/j.1475-4754.2009.00458.x.
URL http://doi.wiley.com/10.1111/j.1475-4754.2009.00458.x

[5] R. Arletti, S. Quartieri, I. C. Freestone, A XANES study of chromophores in archaeological glass, Applied Physics A 111 (1) (2013) 99–108. doi:10.1007/s00339-012-7341-4.
URL http://link.springer.com/10.1007/s00339-012-7341-4http://www.springerlink.com/index/10.1007/s00339-012-7341-4

[6] S. Cagno, G. Nuyts, S. Bugani, K. De Vis, O. Schalm, J. Caen, L. Helfen, M. Cotte, P. Reischig, K. Janssens, Evaluation of manganese-bodies removal in historical stained glass windows via SR-μ-XANES/XRF and SR-μ-CT, Journal of Analytical Atomic Spectrometry 26 (12) (2011) 2442. doi:10.1039/c1ja10204d.
URL http://xlink.rsc.org/?DOI=c1ja10204d

[7] A. Ceglia, G. Nuyts, S. Cagno, W. Meulebroeck, K. Baert, P. Cosyns, K. Nys, H. Thienpont, K. Janssens, H. Terryn, A XANES study of chromophores: the case of black glass, Analytical Methods 6 (8) (2014) 2662. doi:10.1039/c3ay42029a.
URL http://xlink.rsc.org/?DOI=c3ay42029a

[8] L. De Ferri, R. Arletti, G. Ponterini, S. Quartieri, XANES, UV-VIS and luminescence spectroscopic study of chromophores in ancient HIMT glass, European Journal of Mineralogy 23 (2011) 969–980. doi:10.1127/0935-1221/2011/0023-2125.
URL http://openurl.ingenta.com/content/xref?genre=article&issn=0935-1221&volume=23&issue=6&spage=969http://eurjmin.geoscienceworld.org/content/23/6/969.short

[9] E. Gliozzo, A. Santagostino Barbone, F. D'Acapito, Waste Glass, Vessels and Window-Panes From Thamusida (Morocco): Grouping Natron-Based Blue-Green and Colourless Roman Glasses, Archaeometry 55 (4) (2013) 609–639. doi:10.1111/j.1475-4754.2012.00696.x.
URL http://doi.wiley.com/10.1111/j.1475-4754.2012.00696.x

[10] W. Klysubun, Y. Thongkam, S. Pongkrapan, K. Won-in, J. T-Thienprasert, P. Dararutana, XAS study on copper red in ancient glass beads from Thailand., Analytical and bioanalytical chemistry 399 (9) (2011) 3033–40. doi:10.1007/s00216-010-4219-1.
URL http://www.ncbi.nlm.nih.gov/pubmed/20890783

[11] I. Nakai, C. Numako, H. Hosono, K. Yamasaki, Origin of the Red Color of Satsuma Copper-Ruby Glass as Determined by EXAFS and Optical Absorption Spectroscopy, Journal of the American Ceramic Society 82 (3) (2004) 689–695. doi:10.1111/j.1151-2916.1999.tb01818.x.
URL http://onlinelibrary.wiley.com/doi/10.1111/j.1151-2916.1999.tb01818.x/abstracthttp://doi.wiley.com/10.1111/j.1151-2916.1999.tb01818.x

[12] S. Quartieri, M. P. Riccardi, B. Messiga, F. Boscherini, The ancient glass production of the Medieval Val Gargassa glasshouse: Fe and Mn XANES study, Journal of Non-Crystalline Solids 351 (37-39) (2005) 3013–3022. doi:10.1016/j.jnoncrysol.2005.06.046.
URL http://linkinghub.elsevier.com/retrieve/pii/S0022309305005211

[13] A. Santagostino Barbone, E. Gliozzo, F. DAcapito, I. Memmi Turbanti, M. Turchiano, G. Volpe, The Sectilia Panels of Faragola (Ascoli Satriano, Southern Italy): a Multi-Analytical Study of the Red, Orange and Yellow Glass Slabs, Archaeometry 50 (3) (2008) 451–473. doi:10.1111/j.1475-4754.2007.00341.x.
URL http://doi.wiley.com/10.1111/j.1475-4754.2007.00341.x

[14] A. J. Berry, H. S. C. O'Neill, K. D. Jayasuriya, S. J. Campbell, G. J. Foran, XANES calibrations for the oxidation state of iron in a silicate glass, American Mineralogist 88 (2003) 967–977.
URL http://ammin.geoscienceworld.org/cgi/content/long/88/7/967

[15] F. Farges, S. Rossano, Y. Lefrère, M. Wilke, G. E. Brown Jr, Iron in silicate glasses: a systematic analysis of pre-edge, XANES and EXAFS features, Physica Scripta T115 (2006) 957–959.
URL http://iopscience.iop.org/1402-4896/2005/T115/288

[16] I. C. Freestone, Glass production in Late Antiquity and the Early Islamic period: a geochemical perspective, in: M. Maggetti, B. Messiga (Eds.), Geomaterials in cultural heritage, Vol. 257, Geological Society, London, Special Publications, 2006, pp. 201–216. doi:10.1144/GSL.SP.2006.257.01.16.
URL http://sp.lyellcollection.org/cgi/doi/10.1144/GSL.SP.2006.257.01.16

[17] C. R. Bamford, Colour generation and control in glass, Elsevier, Amsterdam, 1977.
URL http://library.dmr.go.th/library/TextBooks/2790.pdf

[18] K. Janssens, Modern Methods for Analysing Archaeological and Historical Glass, John Wiley & Sons Ltd, Oxford, UK, 2013. doi:10.1002/9781118314234.
URL http://doi.wiley.com/10.1002/9781118314234

[19] F. Farges, Y. Lefrère, S. Rossano, A. Berthereau, G. Calas, G. E. Brown Jr, The effect of redox state on the local structural environment of iron in silicate glasses: a combined XAFS spectroscopy, molecular dynamics, and bond valence study, Journal of Non-Crystalline Solids 344 (3) (2004) 176–188. doi:10.1016/j.jnoncrysol.2004.07.050.
URL http://linkinghub.elsevier.com/retrieve/pii/S002230930400599X

[20] W. E. Jackson, F. Farges, M. Yeager, P. A. Mabrouk, S. Rossano, G. A. Waychunas, E. I. Solomon, G. E. Brown Jr, Multi-spectroscopic study of Fe(II) in silicate glasses: Implications for the coordination environment of Fe(II) in silicate melts, Geochimica et Cosmochimica Acta 69 (17) (2005) 4315–4332. doi:10.1016/j.gca.2005.01.008.
URL http://linkinghub.elsevier.com/retrieve/pii/S0016703705000530

[21] M. Wilke, F. Farges, G. M. Partzsch, C. Schmidt, H. Behrens, Speciation of Fe in silicate glasses and melts by in-situ XANES spectroscopy, American Mineralogist 92 (1) (2007) 44–56. doi:10.2138/am.2007.1976.
URL http://ammin.geoscienceworld.org/cgi/doi/10.2138/am.2007.1976

[22] A. Ceglia, W. Meulebroeck, P. Cosyns, K. Nys, H. Terryn, H. Thienpont, Colour and Chemistry of the Glass Finds in the Roman Villa of Treignes, Belgium, Procedia Chemistry 8 (2013) 55–64. doi:10.1016/j.proche.2013.03.008.
URL http://dx.doi.org/10.1016/j.proche.2013.03.008

[23] D. Michaelides, Ayioi Pente at Yeroskipou. A new early christian site in Cyprus, Musiva et Sectilia 1 (2005) 185–198.

[24] A. Ceglia, P. Cosyns, K. Nys, H. Terryn, H. Thienpont, W. Meulebroeck, Submitted. Late Antique glass distribution and consumption in Cyprus: a chemical study, Journal of Archaeological Science.

[25] A. Ceglia, Shedding light on the glass industry of ancient

Cyprus: archaeological questions, methodology and preliminary results, in: V. Kassianidou, M. Dikomitou-Eliadou (Eds.), The NARNIA Project: Integrating Approaches to ancient material studies, Nicosia, 2014, pp. 85–93.

[26] J. H. Pratt, On the determination of ferrous iron in silicates, American Journal of Science s3-48 (284) (1894) 149–151. doi:10.2475/ajs.s3-48.284.149.
URL http://www.ajsonline.org/cgi/doi/10.2475/ajs.s3-48.284.149

[27] A. Silvestri, G. Molin, G. Salviulo, Roman and medieval glass from the Italian area: bulk characterization and relationships with production technologies, Archaeometry 47 (4) (2005) 797–816. doi:10.1111/j.1475-4754.2005.00233.x.
URL http://onlinelibrary.wiley.com/doi/10.1111/j.1475-4754.2005.00233.x/fullhttp://doi.wiley.com/10.1111/j.1475-4754.2005.00233.x

[28] K. Govindaraju, 1994 Compilation of working values and descriptions for 383 geostandards., Geostandards Newsletter 118 (July) (1994) 1–158.

[29] A. Zoleo, M. Brustolon, A. Barbon, A. Silvestri, G. Molin, S. Tonietto, Fe(III) and Mn(II) EPR quantitation in glass fragments from the palaeo-Christian mosaic of St. Prosdocimus (Padova, NE Italy): Archaeometric and colour correlations, Journal of Cultural Heritagedoi:10.1016/j.culher.2014.07.005.
URL http://linkinghub.elsevier.com/retrieve/pii/S1296207414001101

[30] W. H. McMaster, N. Kerr Del Grande, J. H. Mallett, J. H. Hubbell, Compilation of X-Ray Cross Sections, Laboratory Lawrence Radiation UCRL-50174 Report National Bureau of Standards, Springfield, VA, 1969.

[31] A. Michalowicz, J. Moscovici, D. Muller-Bouvet, Karine Provost, MAX: Multiplatform Applications for XAFS, Journal of Physics: Conference Series 190 (2009) 012034. doi:10.1088/1742-6596/190/1/012034.
URL http://stacks.iop.org/1742-6596/190/i=1/a=012034?key=crossref.07961b8534102712038adab5c7c01b75

[32] B. Ravel, M. Newville, ATHENA, ARTEMIS, HEPHAESTUS: data analysis for X-ray absorption spectroscopy using IFEFFIT., Journal of synchrotron radiation 12 (Pt 4) (2005) 537–41. doi:10.1107/S0909049505012719.
URL http://www.ncbi.nlm.nih.gov/pubmed/15968136

[33] W. Meulebroeck, K. Baert, H. Wouters, P. Cosyns, A. Ceglia, S. Cagno, K. Janssens, K. Nys, H. Terryn, H. Thienpont, The identification of chromophores in ancient glass by the use of UV-VIS-NIR spectroscopy, in: F. Berghmans, A. G. Mignani, C. A. van Hoof (Eds.), Proc. SPIE 7726, Vol. 7726, SPIE, Brussels, 2010, p. 77260D. doi:10.1117/12.853666.
URL http://proceedings.spiedigitallibrary.org/proceeding.aspx?doi=10.1117/12.853666http://proceedings.spiedigitallibrary.org/proceeding.aspx?articleid=749647

[34] J.-S. Jeoung, W. H. Poisl, M. C. Weinberg, G. L. Smith, H. Li, Effect of Oxidation State of Iron on Phase Separation in Sodium Silicate Glasses, Journal of the American Ceramic Society 84 (8) (2004) 1859–1864. doi:10.1111/j.1151-2916.2001.tb00927.x.
URL http://onlinelibrary.wiley.com/doi/10.1111/j.1151-2916.2001.tb00927.x/abstracthttp://doi.wiley.com/10.1111/j.1151-2916.2001.tb00927.x

[35] W. A. Weyl, Coloured Glass, Society of Glass Technology, Sheffield, 1976.

[36] C. Russel, Iron oxide-doped alkali-lime-silica glasses. Part 1. EPR investigations, GLASTECHNISCHE BERICHTE 66 (1993) 68–74.

[37] M. Newville, Fundamentals of XAFS, Reviews in Mineralogy and Geochemistry 78 (1) (2014) 33–74. doi:10.2138/rmg.2014.78.2.
URL http://streaming.lehigh.edu/rm/dept/IMI/VirtualGlassCourse/SuppReading/Tutorials.pdf

[38] R. Arletti, G. Vezzalini, C. Fiori, M. Vandini, Mosaic Glass From St Peter'S, Rome: Manufacturing Techniques and Raw Materials Employed in Late 16th-Century Italian Opaque Glass, Archaeometry 53 (2) (2011) 364–386. doi:10.1111/j.1475-4754.2010.00538.x.
URL http://doi.wiley.com/10.1111/j.1475-4754.2010.00538.x

[39] T. T. Volotinen, J. M. Parker, P. A. Bingham, Concentrations and site partitioning of Fe2+ and Fe3+ ions in a sodalimesilica glass obtained by optical absorbance spectroscopy, Physics and Chemistry of Glasses: European Journal of Glass Science and Technology Part B 49 (5) (2008) 258–270.
URL http://www.ingentaconnect.com/content/sgt/pcg/2008/00000049/00000005/art00004

[40] S. P. Singh, a. Kumar, Molar extinction coefficients of the cupric ion in silicate glasses, Journal of Materials Science 30 (11) (1995) 2999–3004. doi:10.1007/BF00349674.

[41] I. C. Freestone, M. Ponting, M. J. Hughes, The origins of Byzantine glass from Maroni Petrera, Cyprus, Archaeometry 44 (2) (2002) 257–272. doi:10.1111/1475-4754.t01-1-00058.
URL http://doi.wiley.com/10.1111/1475-4754.t01-1-00058

[42] M. Wilke, F. Farges, P. E. Petit, Oxidation state and coordination of Fe in minerals: An Fe K-XANES spectroscopic study, American Mineralogist 86 (1998) (2001) 714–730.
URL http://ammin.geoscienceworld.org/content/86/5-6/714.short

[43] G. Nuyts, S. Cagno, K. Hellemans, G. Veronesi, M. Cotte, K. Janssens, Study of the Early Stages of Mn Intrusion in Corroded Glass by Means of Combined SR FTIR/μXRF Imaging and XANES Spectroscopy, Procedia Chemistry 8 (2013) 239–247. doi:10.1016/j.proche.2013.03.030.
URL http://www.sciencedirect.com/science/article/pii/S1876619613000314

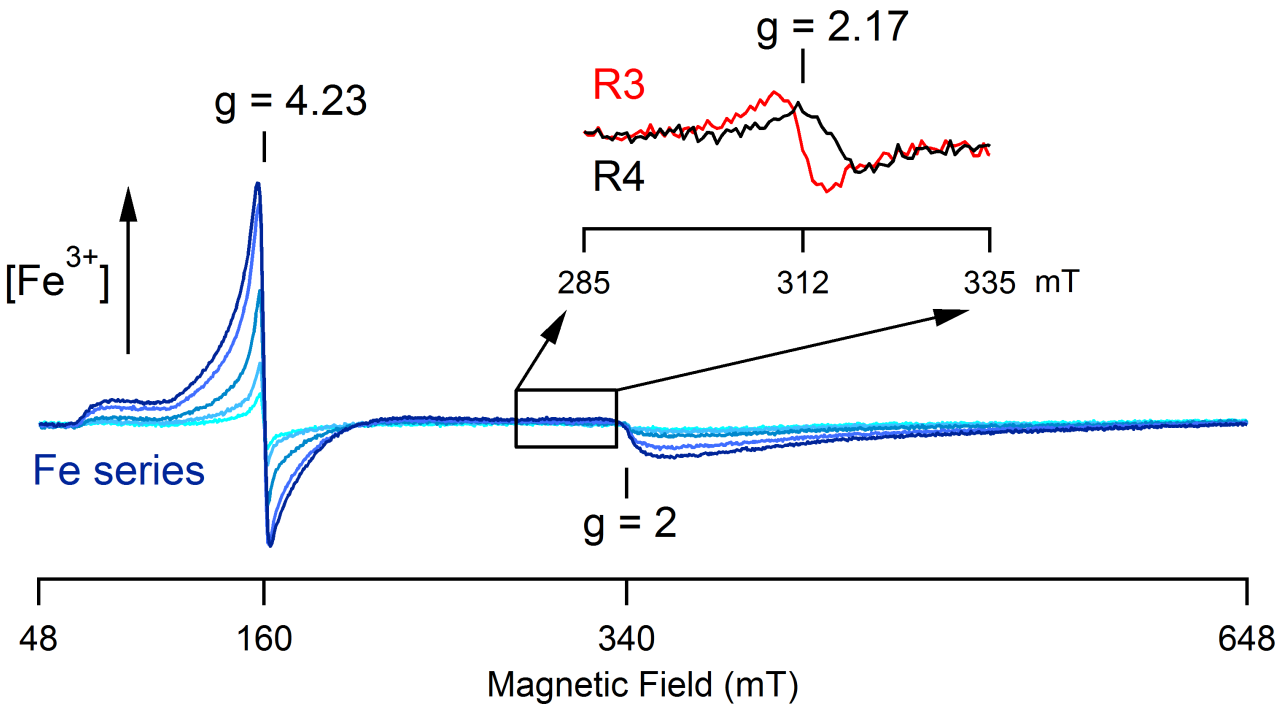

Figure 1: EPR spectra of the Fe-series exhibit two main features at 160 and 340 mT. The first one is due to Fe^{3+} in low symmetry sites, while the second one to Fe^{3+} sites with higher symmetry. Two samples, R3 and R4, have a peculiar feature at 312 mT.

Table 1: Composition of the Fe- and R-series glasses, presented as oxide concentrations (wt%), obtained by XRF and the Fe redox ratio provided by AGC Glass Europe. The Fe-series consists of iron doped soda-lime-silica glasses synthesised with increasing concentration of iron. They were melted at 1550° C under inert N_2 atmosphere. The Fe3 glass was used as base glass to produce the R-series of glasses manufactured under different redox conditions. The R-series was analysed only for iron and sulphur.

	Fe0	Fe1	Fe2	Fe3	Fe4	R1	R2	R3	R4	R5
Al_2O_3	3.152	3.219	3.168	3.168	3.162					
Fe_2O_3	0.062	0.113	0.249	0.543	0.803	0.559	0.543	0.567	0.537	0.533
TiO_2	0.015	0.015	0.016	0.015	0.016					
Na_2O	15.45	15.48	15.42	15.36	15.38					
K_2O	0.038	0.038	0.037	0.035	0.038					
MgO	0.16	0.13	0.13	0.13	0.13					
CaO	8.2	8.31	8.36	8.19	8.18					
SO_3	0.026	0.025	0.027	0.027	0.028	0.037	0.032	0.028	0.024	0.021

Table 2: Comparison of determined values of Fe^{2+} with different analytical techniques. The values obtained by wet chemistry are used as reference. The data are tested by EPR and XANES, for which we show also the centroids. Wet chemistry data are used to and used to calibrate optical spectroscopy. We report the absorbance measured at 1100 nm and the Fe^{2+} in elemental wt% obtained by optical spectroscopy after calibration. *na* = not analysed.

sample	Fe^{2+} determination		XANES		UV-vis-NIR	
	Wet chem	EPR	centroid	Fe^{2+}	A_{1100nm}	Fe^{2+}
Fe0	0.020	0.015	na		0.0109	0.020
Fe1	0.037	0.017	na		0.0279	0.034
Fe2	0.059	0.031	na		0.0649	0.064
Fe3	0.102	0.083	7113.59	0.101	0.1297	0.117
Fe4	0.134	0.153	7113.67	0.120	0.1642	0.145
R1	0.096	0.060	7113.68	0.081	0.0907	0.085
R2	0.101	0.066	7113.70	0.074	0.0942	0.088
R3	0.162	0.172	7113.37	0.163	0.2135	0.185
R4	0.188	0.151	7113.46	0.131	0.2207	0.191
R5	0.296	0.260	7112.88	0.272	0.3400	0.288

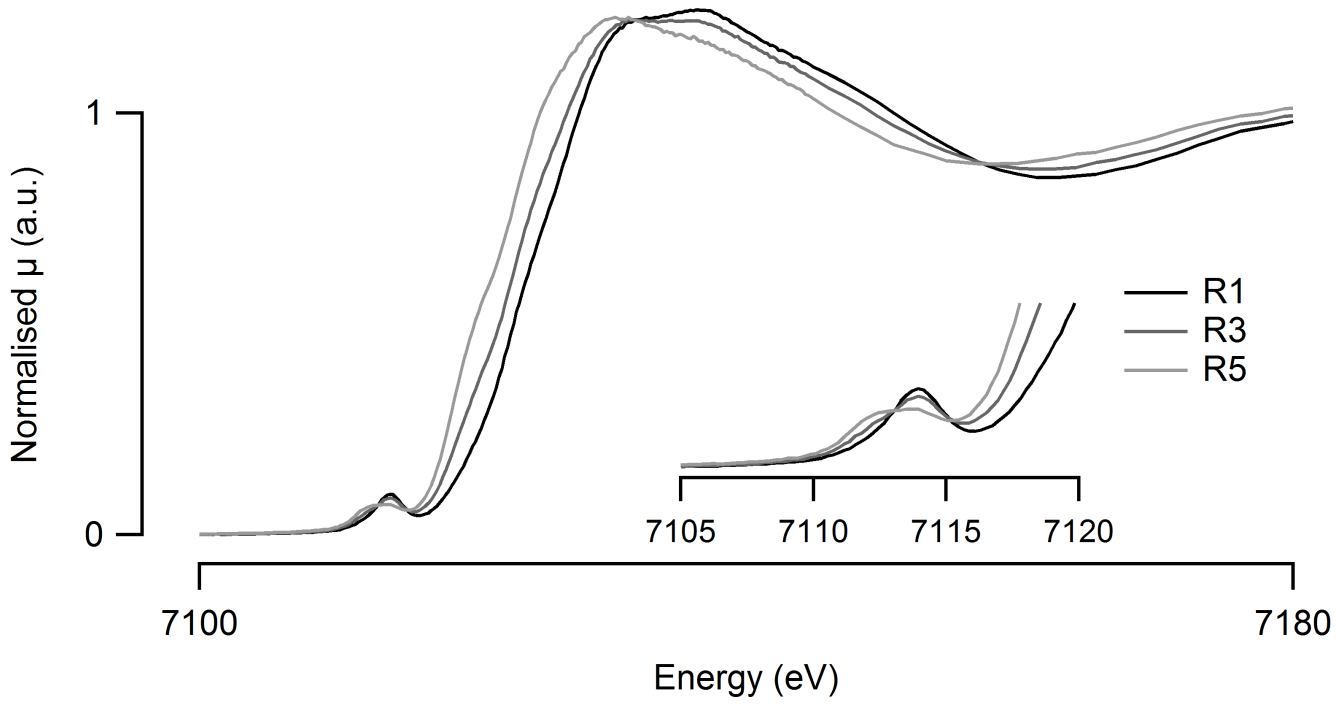

Figure 2: Fluorescence XANES spectra of three lab-made model glasses, R1, R3 and R5. Changing from reduced to oxidised the pre-edge and the edge energies are shifted towards higher values. In the inset a zoom of the pre-edge feature is shown.

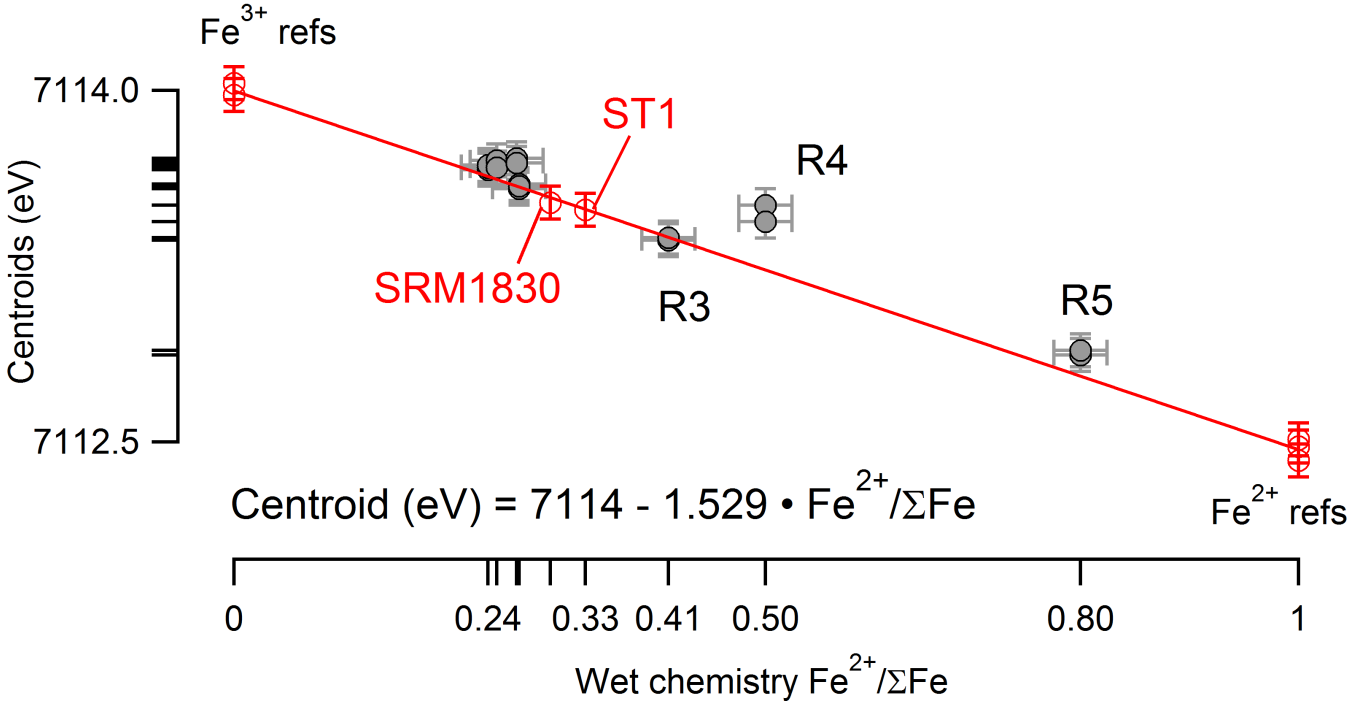

Figure 3: The centroid positions of mineral and glasses references are used to build a straight correlation line. Plotting the centroid positions of the glasses of the Fe- and R-series against the values of $Fe^{2+}/\Sigma Fe$ obtained by wet chemistry, we note that the linear correlation is valid. Sample R4 is the only one off the correlation line likely due to its inhomogeneity. Note that all repeated scans on the model glasses are reported.

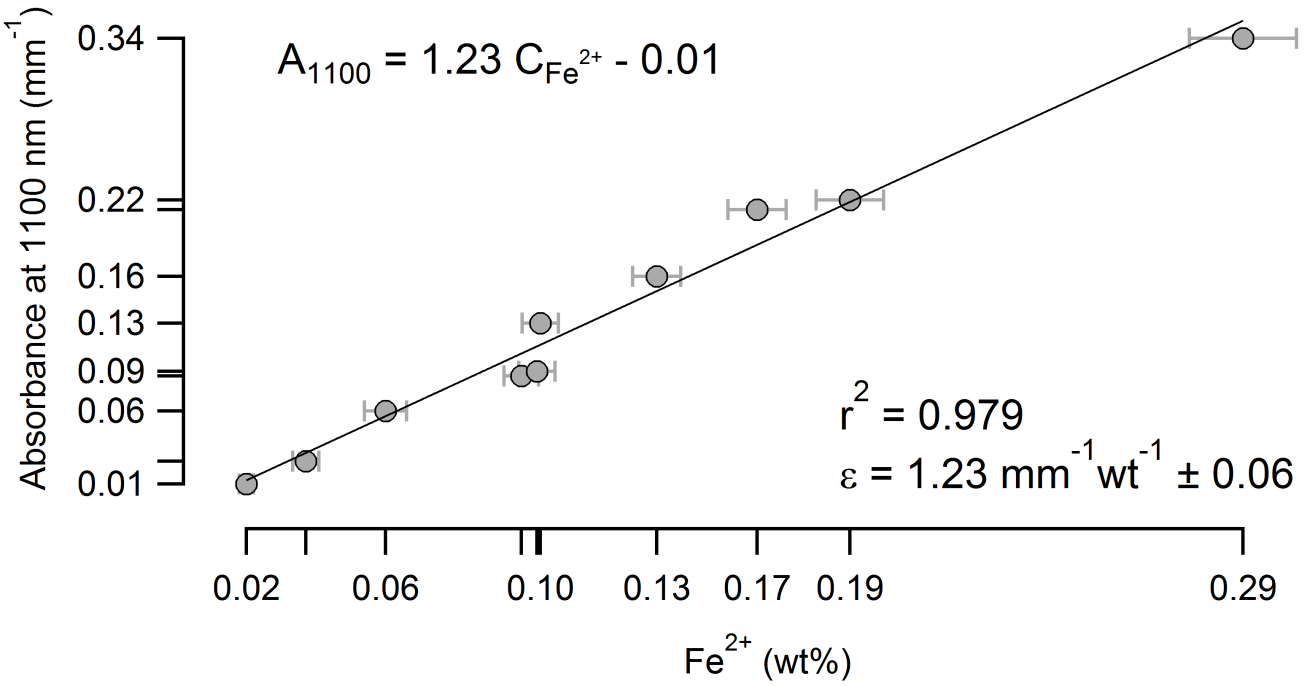

Figure 4: The absorbance of glass at 1100 nm is due to Fe^{2+} ions. By applying the Lambert-Beer law it is possible to obtain a correlation line between the absorbance and Fe^{2+} concentration and obtain the linear absorption coefficient ϵ. The values of Fe^{2+} for the calibration are determined by wet chemistry and reported in elemental wt%.

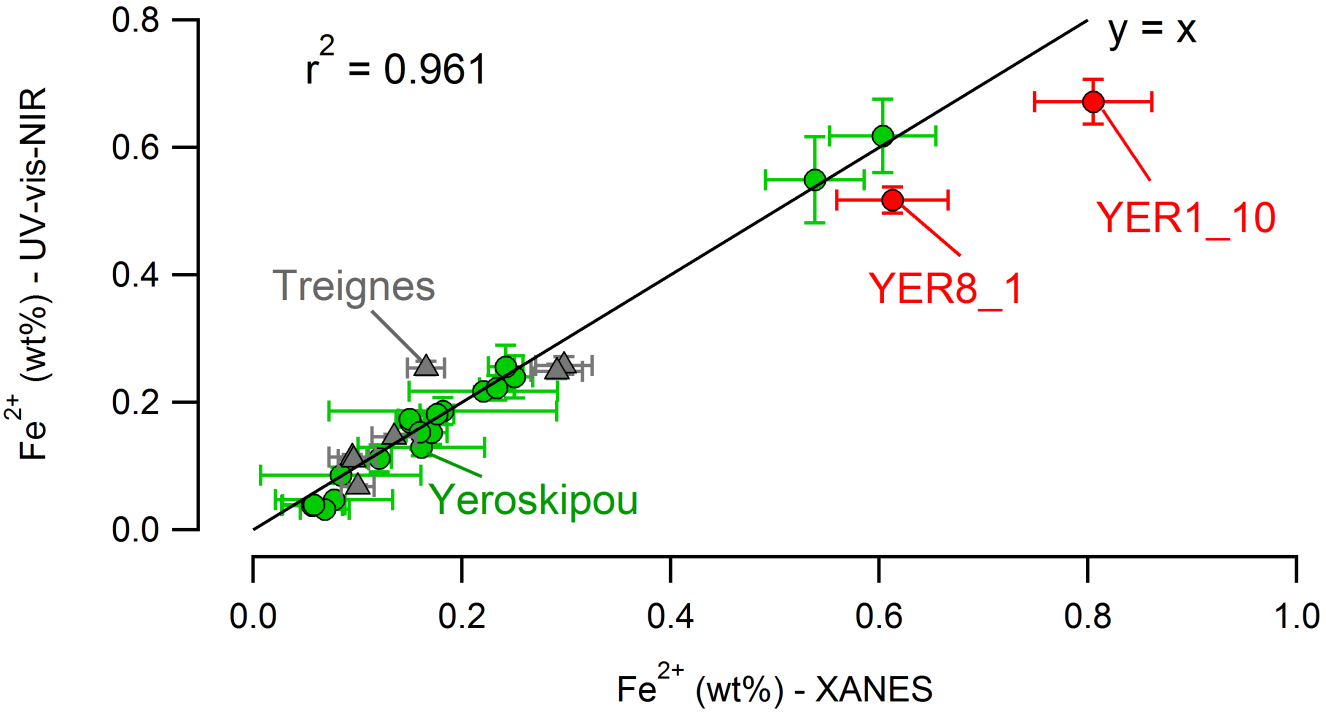

Figure 5: Comparing the Fe^{2+} in archaeological glasses determined by XANES and optical spectroscopy, we notice that there is a good agreement between the two methods. Only two samples, YER1_10 and YER8_1, are clearly off because the optical measurement was hamperd by their low transmission at 1100 nm. The values of Fe^{2+} are reported in elemental wt%.

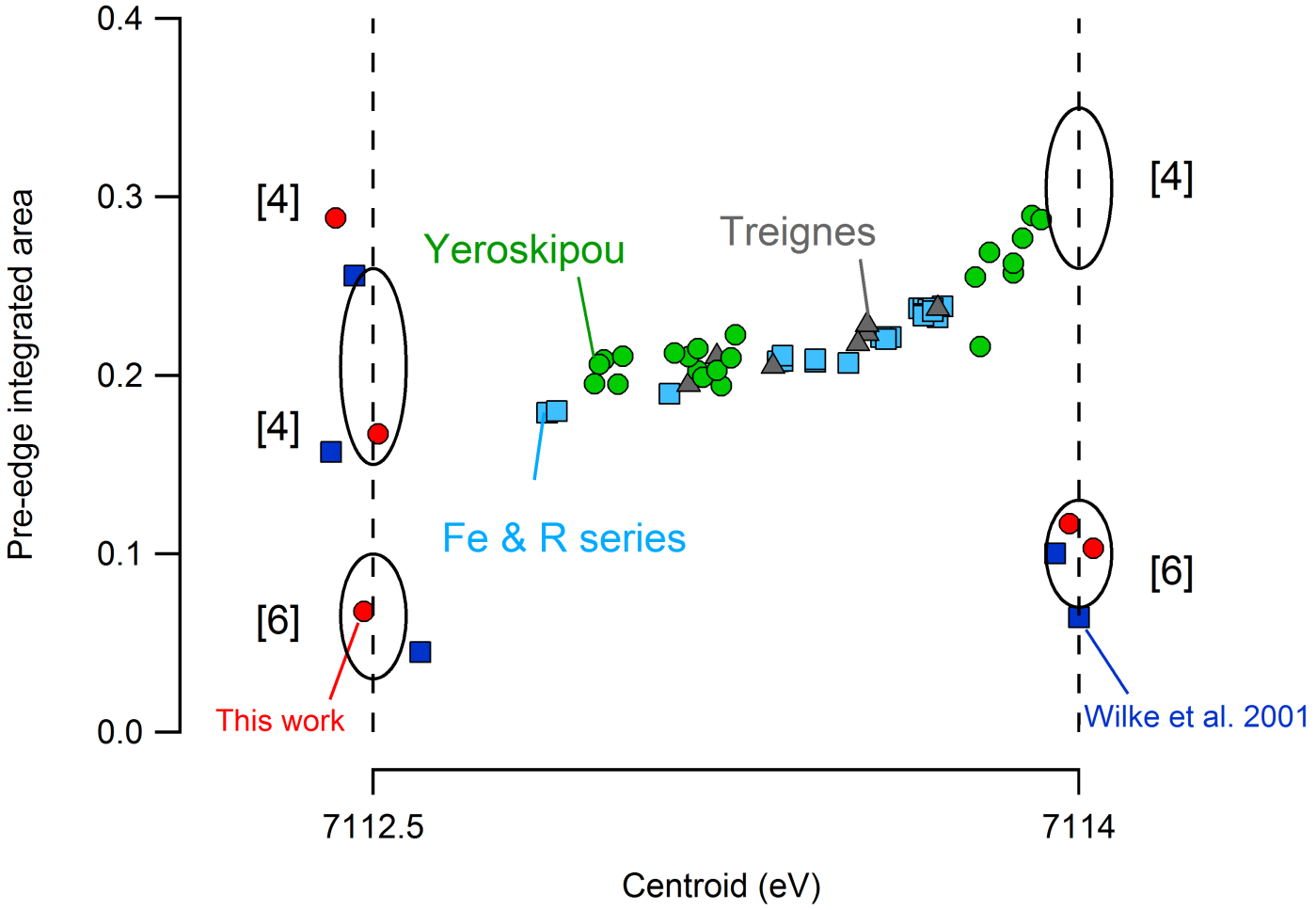

Figure 6: The pre-edge area is plotted against the centroid position in order to describe the coordination geometry surrounding the iron atoms. The data measured on the same minerals by Wilke et al [42] are also reported. The circles describe the expected position of octahedral, [6], and tetrahedral, [4], Fe^{3+} and Fe^{2+} compounds. The values have been postulated considering literature data.

Table 3: Centroid and integrated area of the pre-edge for mineral and glass references. The values reported by Wilke et al. [42] are also shown. The energy disagreement is due to a different energy calibration.

		This work		Wilke et al. 2001 [42]	
Reference	Coordination	Centroid	Pre-edge Area	Centroid	Pre-edge Area
Aegerine	$^{[6]}Fe^{3+}$	7114.03	0.103	7113.51	0.100
Epidote	$^{[6]}Fe^{3+}$	7113.98	0.117	7113.56	0.064
Chromite	$^{[4]}Fe^{2+}$	7112.51	0.167	7111.97	0.157
Hercynite	$^{[4]}Fe^{2+}$	7112.42	0.288	7112.02	0.256
$FeSO \cdot 4\,H_2O$	$^{[6]}Fe^{2+}$	7112.48	0.068	7112.16	0.045
SRM1830	70% Fe^{2+}	7113.52	0.217		
ST1	33% Fe^{2+}	7113.49	0.223		

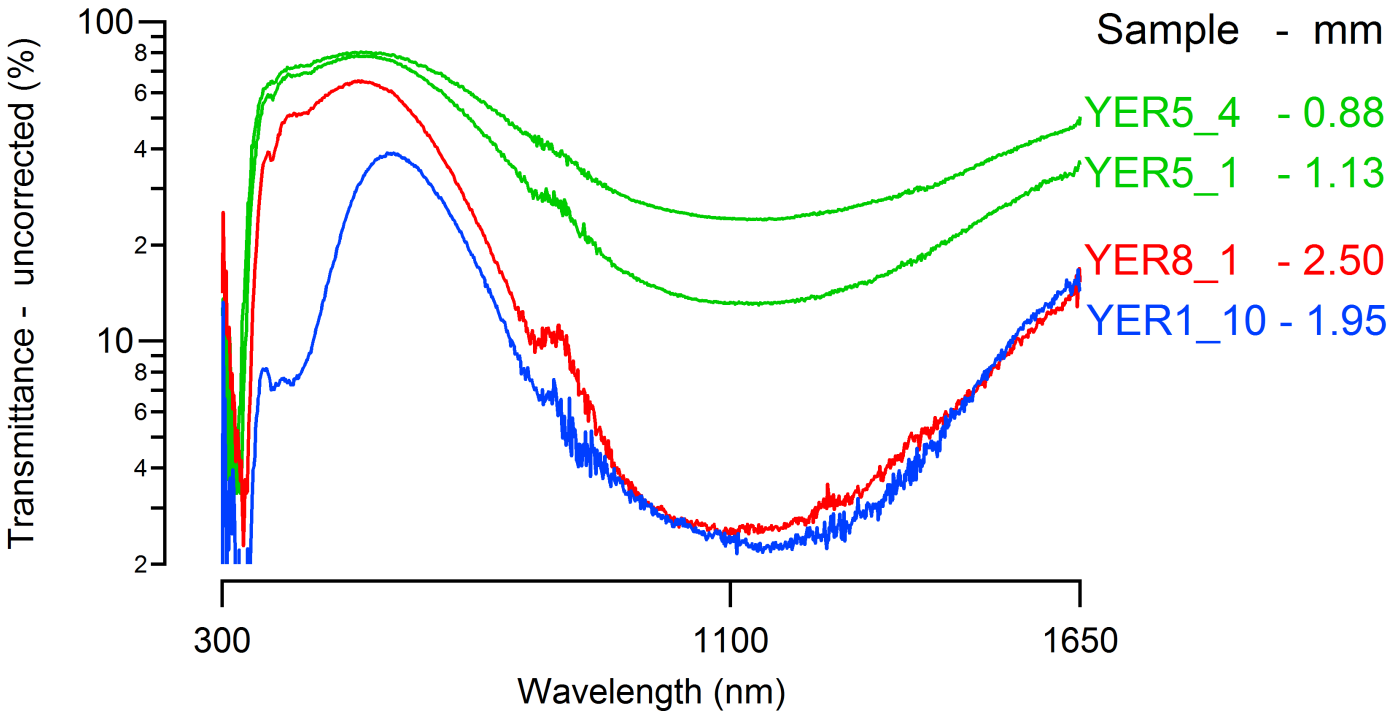

Figure 7: The uncorrected transmission spectra for the archaeological samples with higher concentration of iron show clearly that the underestimation of Fe^{2+} in samples YER1_10 and YER8_1 is due to the lack of transmission at 1100 nm. The feature at 830 nm is an instrumental artefact due to the switch between detectors.

Supplementary Table: Evaluation of the Fe^{2+} content in archaeological glasses. All values of Fe^{2+} and Fe_{tot} are given in elemental wt%, while the centroid is in eV.

	XANES			UV vis NIR			EPMA
Sample	Centroid	$Fe^{2+}/\Sigma Fe$	Fe^{2+}	A_{1100nm}	$Fe^{2+}/\Sigma Fe$	Fe^{2+}	Fe_{tot}
YER1_7	7113.81	0.12	0.16	0.145	0.10	0.13	1.32
YER1_10	7112.99	0.66	0.81	0.811	0.55	0.67	1.22
YER2_1	7113.78	0.14	0.22	0.253	0.14	0.22	1.56
YER2_3	7113.86	0.09	0.06	0.033	0.06	0.04	0.63
YER3_1	7113.90	0.06	0.08	0.044	0.04	0.05	1.23
YER3_2	7113.79	0.14	0.07	0.026	0.06	0.03	0.51
YER3_3	7113.88	0.08	0.18	0.215	0.08	0.19	2.38
YER4_4	7113.86	0.09	0.06	0.034	0.06	0.04	0.65
YER4_5	7113.02	0.64	0.23	0.260	0.61	0.22	0.37
YER4_8	7113.19	0.53	0.17	0.174	0.47	0.15	0.32
YER4_9	7113.24	0.49	0.15	0.193	0.55	0.17	0.30
YER5_1	7113.17	0.54	0.60	0.745	0.55	0.62	1.12
YER5_4	7113.20	0.52	0.54	0.661	0.53	0.55	1.03
YER5_8	7113.27	0.48	0.12	0.124	0.44	0.11	0.25
YER6_1	7113.03	0.63	0.15	0.199	0.73	0.17	0.24
YER6_3	7113.23	0.50	0.18	0.209	0.52	0.18	0.35
YER6_6	7113.92	0.05	0.08	0.091	0.05	0.09	1.68
YER7_5	7112.98	0.66	0.25	0.281	0.64	0.24	0.38
YER7_9	7113.14	0.56	0.16	0.175	0.54	0.15	0.29
YER8_1	7113.19	0.53	0.61	0.622	0.45	0.52	1.16
YER8_3	7112.97	0.67	0.24	0.301	0.71	0.26	0.36
TR1_2	7113.23	0.50	0.30	0.303	0.43	0.26	0.59
TR1_3	7113.35	0.42	0.17	0.298	0.65	0.25	0.39
TR1_5	7113.55	0.29	0.10	0.069	0.20	0.07	0.34
TR1_6	7113.17	0.54	0.29	0.292	0.46	0.25	0.54
TR2_3	7113.70	0.19	0.09	0.127	0.23	0.11	0.49
TR2_7	7113.55	0.29	0.13	0.165	0.32	0.15	0.46
TR2_9	7113.53	0.31	0.10	0.121	0.35	0.11	0.31